Ternary Cobalt−Copper−Niobium Catalysts for the Selective CO Hydrogenation to Higher Alcohols

Yizhi Xiang,[†,‡] Roland Barbosa,[†,‡] Xiaonian Li,[§] and Norbert Kruse*[,†,‡]

[†]Chemical Physics of Materials (Catalysis-Tribology), Université Libre de Bruxelles, Campus Plaine, CP 243, 1050 Brussels, Belgium

[‡]Voiland School of Chemical Engineering and Bioengineering, Washington State University, P.O. Box 646515, Pullman, Washington 99164-6515, United States
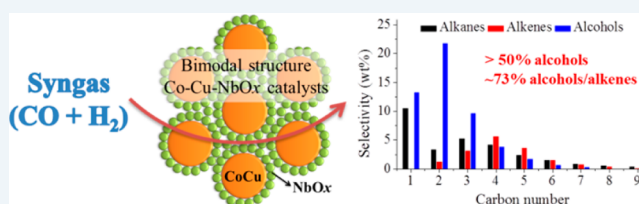
[§]Industrial Catalysis Institute of Zhejiang University of Technology, State Key Laboratory Breeding Base of Green Chemistry Synthesis Technology, Hangzhou, Zhejiang 310014, People's Republic of China

Ⓢ *Supporting Information*

ABSTRACT: Novel "CoCuNb" ternary catalysts with bimodal nanosized particle structure, in the absence of a generic support material, were designed and successfully tested in higher alcohol production via CO hydrogenation. The selectivities to primary alcohols with an optimized C_2-C_5 slate usually exceeded the 50 wt % level, and the combined selectivities to 1-alcohols/1-alkenes reached up to ∼73 wt % for CO conversions ranging between ∼5% and nearly 20%.

The bimodal nanosized particle distribution, achieved through oxalate coprecipitation, contained Co−Cu particles with sizes ranging from 25 to 40 nm. Smaller particles between 4 and 8 nm were identified as Nb oxides and played the role of a structural dispersant ("spacer") and promoter of 1-alcohol/1-olefin production. X-ray photoelectron spectroscopy revealed NbO_x to contain major amounts of species with Nb in the 4+ oxidation state.

KEYWORDS: *CO hydrogenation, C_2-C_5 alcohols, CoCuNb, bimodal structure, SMSI effect*

■ INTRODUCTION

The "oxo" synthesis (or "hydroformylation") transforms a C_n terminal olefin into a C_{n+1} aldehyde using CO and hydrogen at high pressures in the liquid phase. While the reaction was considered to occur at the surface of a solid Co-based catalyst at the time of its discovery by Roelen in 1938,[1] it turned out to be a case of homogeneous catalysis involving tetracarbonyl cobalt hydride, $HCo(CO)_4$.[2] Nowadays, ligand-modified organometallic Co and Rh catalysts are used in large-scale industrial applications. Most aldehydes of the C_8-C_{14} range are turned into "fatty" alcohols by subsequent hydrogenation and serve as feedstock for the production of detergents, lubricants, and plasticizers. The prospect of producing such oxygenates with high selectivity in a "one-step−one-pot" heterogeneous process using CO hydrogenation at moderate pressures according to the Fischer−Tropsch (FT) technology was demonstrated only quite recently.[3] Different from hydroformylation, where the (reversible) transformation from an 18e to a 16e organometallic complex creates "empty" metal orbitals for π binding the terminal olefin, the question of the nature of the catalytically active site in the heterogeneous case of CO hydrogenation, without the involvement of a target olefin, remains a matter of debate.[4] Recent experimental studies using atom counting in relaxation-type studies, though, called into question the view that metallic sites are being involved at all,[5] in agreement with other reports in the literature.[6]

The formation of oxygenates during heterogeneous CO hydrogenation has actually already been observed by Fischer and Tropsch.[7] Since the 1930s, various FT-related studies reported the production of "iso" or "oxo" alcohols other than methanol,[8] albeit with rather limited selectivity. Following these earlier studies, with the incentive of generating valuable fuel additives, the Institut Français du Pétrole (IFP) devoted considerable efforts in the 1970s to synthesize "higher" alcohols of up to C_6 with mixed *iso* and *n* constitution using what they called "modified methanol catalysis". Indeed, their catalysts were based on CoCu "alloys"—note that the solubility of one metal in the other is rather limited in this case—and led to considerable alcohol selectivity employing $CO/CO_2−H_2$ feeds in an operational manner similar to the industrial methanol synthesis.[9] Despite a considerable number of reports as patents[10] or in the open literature[11] the reproducibility in both the preparation and performance stability of such CoCu-based catalysts has remained an issue up until now.[11a,12d] The conceptual approach of combining transition metals with both C−O bond-breaking (Co) and bond-conserving (Cu) capability yet also seems to be a driving force for ongoing research on such higher alcohol synthesis with these metals.[12]

Different from the IFP patent claims which emphasize the necessity of producing a homogeneous distribution of Co metal across the catalyst particles,[10] an atomic-scale mixing in nanosized particles of Co and Cu, within the limits imposed by the thermodynamics, was envisioned and achieved in our laboratory by coprecipitating both metals into a common oxalate precursor structure.[3b,5,13] Such catalyst preparations were free of a classical support and resulted in stable catalytic performance, after activation, once the oxalate coprecipitation included Mn as a third metal. The thermal decomposition of such mixed oxalate precursors resulted in core@shell structured metal nanoparticles, with Co forming the core and all three elements being present in an otherwise Cu dominated shell of about 1−3 nm thickness, depending on the actual size of the particles. Moreover, metal oxide particles were identified, with Mn_5O_8 forming the most significant oxide phase.[3b]

The obvious occurrence of metallic nanoparticles with favorable core@shell structure and their concurrent association with metal oxide particles in which the metal ions coexist in different valence states suggest strong metal support interaction (SMSI) effects to be in operation during oxygenate production from syngas. Reducible metal oxides such as niobia and titania may therefore be considered similarly good candidates to tune the reaction. Previous research with Co/Nb_2O_5 catalysts demonstrated niobia to increase the selectivity to long-chain products.[14] With this background we developed a new type of "CoCuNb" catalyst via oxalate precursor formation which, after hydrogen-assisted activation and in the absence of a generic support material, turned out to produce primary alcohols (and olefins) with high selectivity. As will be reported here, such "CoCuNb" catalysts turned out to contain a Nb oxide phase in the form of NbO_2 nanoparticles acting as dispersant for Co−Cu metallic particles. Actually, a bimodal particle size distribution was found consisting of smaller NbO_2 (4−8 nm) and larger Co−Cu nanoparticles (25−40 nm). Different from the "CoCuMn" ternary metal combination, which allowed an optimization of the $C_8−C_{14}$ 1-alcohol/1-olefin selectivities, we demonstrate in the present paper that the C_{2+} range up to C_7 may be favored by "CoCuNb" formulations at otherwise negligible CO_2 levels and relatively little methanol formation.

■ EXPERIMENTAL SECTION

Catalyst Preparation. Binary Co−Cu oxalates were coprecipitated by quickly adding a mixed solution of Co-$(NO_3)_2 \cdot 6H_2O$ and $Cu(NO_3)_2 \cdot 3H_2O$ to an excess of oxalic acid, $H_2C_2O_4 \cdot 2H_2O$, with vigorous stirring using acetone as solvent. After removal of the supernatant acetone the precipitate was centrifuged, dried overnight at 110 °C, and finally crushed and sieved so as to obtain a size fraction between 125 and 250 μm for characterization and high-pressure catalytic investigations.

Ternary Co−Cu−Nb oxalates were precipitated stepwise. First, a mixture containing an excess of oxalic acid and ammonium niobate(V) oxalate precipitate was prepared by adding an aqueous solution of ammonium niobate(V) oxalate to an oxalic acid solution in acetone with vigorous stirring. Second, a mixed solution of $Co(NO_3)_2 \cdot 6H_2O$ and $Cu(NO_3)_2 \cdot 3H_2O$ in acetone was added quickly to the preprepared mixture, thus making use of an entrainment effect (ammonium niobate(V) oxalate is not soluble in acetone). The solution was stirred for at least 2 h until the color of the precipitates appeared to be homogeneous. Finally, the precipitate was washed, dried, and crushed according to the same procedure as described in the case of binary Co−Cu oxalates. The prepared

catalysts were denoted as $Co_xCu_yNb_z$, in which x, y, and z represent the relative atomic amounts of Co, Cu, and Nb, respectively. It is noted that in both cases the supernatant solutions after precipitation were clear and transparent.

The mixed-metal oxalate or hybrid precursors were treated thermally in the presence of hydrogen either directly in the high-pressure flow reactor (0.1 MPa H_2, 50 mL min^{-1} at 370 °C for 1 h) for catalytic testing or in an atmospheric-pressure U-type flow reactor for characterization. Oxalates decomposed either quantitatively to metal, as applied to Cu, or to Me/MeO_x, as was the case for Co and Nb. Activation of the oxalate was usually performed in a temperature-programmed manner (10% H_2 in Ar as vector gas at a volumetric flow rate of 30 mL min^{-1} using a ramp of 3 °C min^{-1} up to 370 °C). Reduced catalysts were pyrophoric and had to be passivated (1% O_2 in Ar at 25 °C, 30 min) before TEM, XRD, and XPS characterization.

Catalyst Characterization. X-ray photoelectron spectroscopy (XPS) studies were carried out in a multimethod UHV system with a base pressure of 5×10^{-11} mbar. Using a nonmonochromated Mg Kα radiation, the X-ray source was operated with an acceleration voltage of 13 kV and an emission current of 10 mA. High-resolution scans were made for Nb 3d, Co 2p, Cu 2p, C 1s, O 1s, and Cu LMM employing a pass energy of 50 eV with a dwell time of 0.1 s and a step size of 0.05 eV. The CasaXPS software was used to subtract the Shirley-type background of the spectra and to deconvolute the signal envelopes into components (mixed Gaussian−Lorentzian lines using a nonlinear least-squares curve-fitting procedure). The C 1s peak at 284.4 eV was used as a reference energy for charge correction. The morphology and particle size distribution of CoCuNb catalysts were determined by a Tecnai G2 F30 S-Twin TEM at an operating voltage of 300 kV.

Catalytic Testing. High-pressure catalytic tests were performed in a fixed-bed plug-flow reactor consisting of a quartz tubule (Φ_{inner} = 7 mm) inserted into a stainless steel housing. A condenser along with a gas−liquid separator was mounted at the reactor outlet. Typically, 1.3 g of oxalate was diluted with up to 2 g of SiC to achieve isothermal plug-flow conditions followed by in situ TPDec in H_2 at 0.1 MPa (50 mL min^{-1}) and 370 °C for 1 h (after oxalate decomposition, the amount of activated catalyst is around 0.5 g). The reactor was subsequently cooled to ambient temperature in flowing hydrogen before adding CO so as to produce a 1.5/1 H_2/CO syngas feed. Metal carbonyls (mainly $Ni(CO)_4$) were removed by passing the CO feed through a zeolite 4A trap at high temperature before introduction into the reactor. Typical flow rates were H_2/CO = 24/16 mL min^{-1}, providing GHSV = 3600 h^{-1} (gas hourly space velocity without including SiC inert). After the system was pressurized to 6 MPa, the temperature was raised first to values between 180 and 200 °C (the exact value depended on the type of catalyst) and kept overnight under these conditions. The final temperatures for the catalytic tests were approached using low heating rates of 1 °C min^{-1}. Catalytic activities and product selectivities were determined after stabilization for at least 12 h. The CO conversion and product selectivities were measured by online GC-MS (Agilent 7890A GC/5975 MS).

■ RESULTS AND DISCUSSION

The catalytic performance of "CoCuNb" was first compared with that of the binary "CoCu" and "CoNb" catalysts. Previous research with binary "CoCu" of varying relative metal amounts

demonstrated a 2/1 ratio to provide the best catalytic performance in terms of activity and alcohol selectivity.[15] Figure 1 provides a comparison in terms of CO conversion,
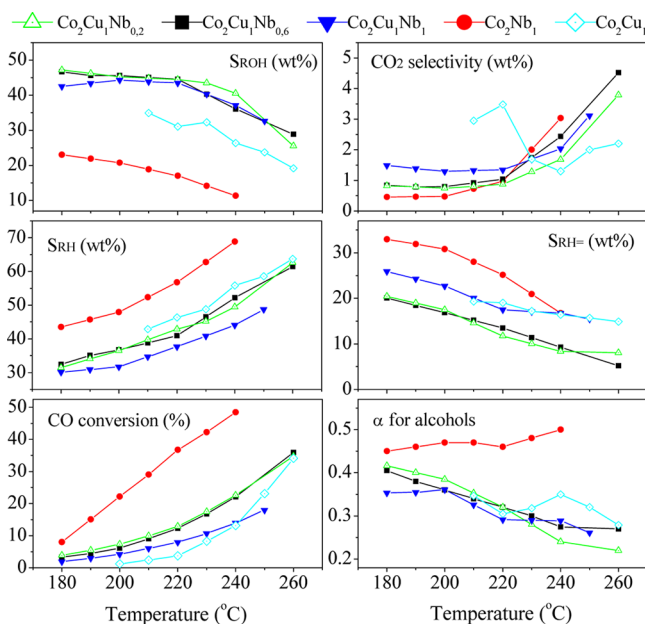

Figure 1. Catalytic performance of Co_2Cu_1, Co_2Nb_1, and $Co_2Cu_1Nb_x$ for CO hydrogenation. Catalytic tests were carried out at p = 60 bar, H_2/CO = 1.5 and total gas flow 40 mL/min. The α-ASF chain lengthening probability was calculated on the basis of the equation $W_n = n(1 - \alpha)^2 \alpha^{n-1}$, where W_n stands for the mass fraction of products containing n carbon atoms. S_{ROH}, S_{RH}, and $S_{RH=}$ represent the selectivities to alcohols, paraffins, and olefins, respectively. The conversion at and below 200 °C is low for Co_2Cu_1 and does not allow determination of the product selectivity.

selectivity to various product classes, and respective Anderson-Schulz−Flory (ASF) chain-lengthening probabilities for Co_2Cu_1, Co_2Nb_1, $Co_2Cu_1Nb_1$, $Co_2Cu_1Nb_{0.6}$ and $Co_2Cu_1Nb_{0.2}$ catalytic formulations as a function of temperature. Generally, the ternary $Co_2Cu_1Nb_x$ catalysts show higher activity and alcohol selectivity (S_{ROH}) in comparison to the binary Co_2Cu_1 catalyst, proving that the presence of Nb promotes the formation of alcohols. The alcohol selectivity, S_{ROH}, increases with decreasing reaction temperatures from 260 to 220 °C, followed by a nearly constant level of at least 40% to nearly 50% at temperatures between 220 and 180 °C for all $Co_2Cu_1Nb_x$ catalysts. Increasing Nb_x relative amounts from x = 0.2 to 1 has almost no influence on the product selectivities and alcohols chain lengthening probability, the latter ranging between 0.3 and 0.4, thus meeting the target of high, though not optimum, selectivity of the C_{2-5} slate (see Figure S1 in the Supporting Information). Terminal olefins which can be converted into primary alcohols using anti-Markovnikov homogeneous hydration[16] are formed by all catalysts; the selectivity increases with decreasing temperatures. $Co_2Cu_1Nb_x$ catalysts turn out to be less selective in this respect than Co_2Nb_1. However, the combined 1-alcohol/1-olefin selectivity remains highest for $Co_2Cu_1Nb_x$ and may reach about 70% in Figure 1. This performance signature applies to low temperatures and comes at the price of quite low CO conversion. Unwanted CO_2 formation is under control and plays no role under these low-temperature reaction conditions.

Summarizing, the results of Figure 1 clearly demonstrate the tradeoff between 1-alcohol/1-olefin selectivity and catalytic activity for decreasing reaction temperatures. The Co_2Nb_1 catalyst is the most active but produces mainly paraffins. The CO conversion at 240 °C is near 50%, but the selectivity to oxygenates (both alcohols and aldehydes) is only ∼10% for this catalyst (the temperature dependence of the CO conversion is rather particular and suggests further kinetic studies which are not within the scope of the present paper). It therefore turns out that the presence of both Co and Cu in "CoCuNb" is mandatory for the selective production of alcohols. We also note that methanol shows a negative deviation from the linear ASF distribution for $Co_2Cu_1Nb_x$ (for a typical ASF plot of alcohols, alkanes, and alkenes over $Co_2Cu_1Nb_{0.2}$ see Figure S2 in the Supporting Information). We do not exclude at present that the site requirements for methanol formation are different from those for initiating chain lengthening. On the other hand, secondary reactions such as aldol-type condensation according to Guerbet[17] or steam reforming would not be compatible with the range of products detected. Additionally, we observe a strongly negative deviation of C_2- and C_3-alkenes from the linear ASF behavior (Figure S2). This observation is not unusual for the Fischer−Tropsch reaction and was the subject of detailed investigations on the basis of chain-length dependent diffusion, readsorption, and reaction. An exponential increase of the paraffin/olefin ratio with increasing carbon number was reported for catalysts leading to wax-type products.[18] This is not the case here, since the ASF chain lengthening probabilities α are too low to produce waxes, and a strict linear ASF behavior was found for C_{3+} olefins. The α values for paraffins (C_{2+}), olefins (C_{3+}), and alcohols (C_{2+}) (see Table S1 in the Supporting Information) increase in the order $\alpha_{alcohols} < \alpha_{alkenes} < \alpha_{alkanes}$. It is felt that the deviations from the ASF behavior for the early homologues of these product classes, in the absence of wax-type compound formation, need further investigation.

The above results demonstrate that the presence of Nb in CoCu enhances both the activity and alcohol selectivity. The $Co_2Cu_1Nb_{0.2}$ formulation seems to perform somewhat better than catalysts with a larger relative Nb amount. To identify the optimum relative amounts of Co and Cu in catalysts with low Nb content, we investigated $Co_xCu_yNb_{0.2}$ ternary systems with x/y ratios ranging from 2/1 to 1/8. The results are shown in Figure 2. Generally, high alcohol selectivities S_{ROH} up to 55 wt % are observed for temperatures between 180 and 240 °C. A further increase of the temperature beyond this range causes a sharp drop in S_{ROH}. This behavior is also observed in Figure 1, and we conclude that any search aimed at balancing the tradeoff between 1-alcohol/1-olefin and catalytic activity is limited to this lower range of temperatures.

The combined 1-alcohol/1-olefin maximum selectivity reaches ∼73 wt % at about 200 °C; however, the CO conversion remains below 10%. Increasing the Co/Cu ratio from 1/8 to 2/1 results in a continuous increase of the conversion but eventually causes a decrease in the terminal alcohol selectivity for Co/Cu (x/y) ratios exceeding 1/2. The best catalyst in terms of alcohol formation turns out to be $Co_1Cu_2Nb_{0.2}$, which provides S_{ROH} values between 43 and 49 wt % at CO conversions ranging from 12 to 21% (see Figure S3 in the Supporting Information for an explicit demonstration of the relation between S_{ROH} or Y_{ROH} and CO conversion). Furthermore, changing the Co/Cu ratios in "CoCuNb" catalysts has almost no effect on the α-ASF chain-lengthening
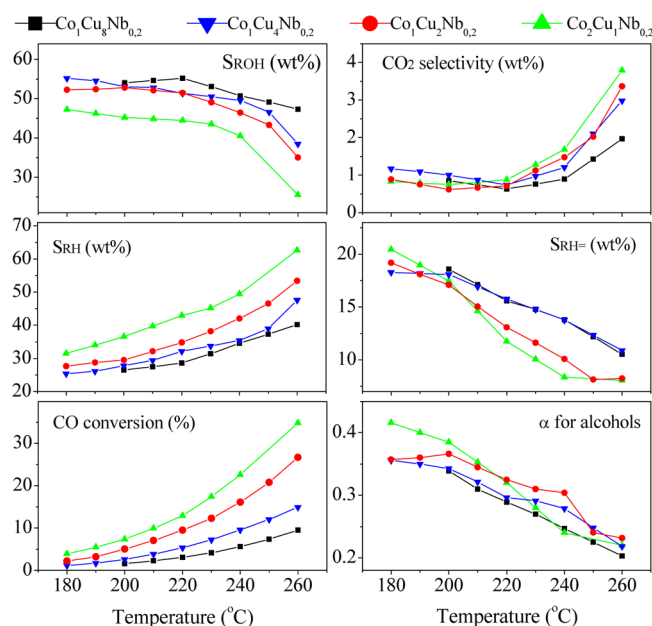
Figure 2. Catalytic performance of $Co_xCu_yNb_{0.2}$ with various Co/Cu relative ratios for CO hydrogenation. See Figure 1 for the reaction conditions.

probability of alcohols. The α values (ranging from 0.2 to ~0.4) increase continuously with decreasing temperatures (except for some fluctuations at low temperatures). Similar to the case for Figure 1, CO_2 formation is insignificant at low temperatures.

Recently Prieto et al.[19] reported on higher alcohols formation over $K-CoCu/MoO_x$ catalysts. From their results, the total alcohol selectivity (not including CO_2) was ~45% C at otherwise <2% CO conversion. Moreover, the CO_2 selectivity in their study was up to 22.4−41.6%. It is also noteworthy that our former studies on "CoCuMo"[20] showed unfavorable CO_2 selectivity similar to that reported by Prieto et al.[19] Furthermore, "CoCuMo", unlike $K-CoCu/MoO_x$, was found to exhibit a double α-ASF distribution of primary alcohols. On comparison of "CoCuNb", subject of the present paper, with $K-CoCu/MoO_x$ in terms of time yield performance, it seems the latter has advantages over "CoCuNb" (27 vs ~3.8 mmol g_{Co+Cu}^{-1} h^{-1}). However, while $K-CoCu/MoO_x$ produces significant amounts of CO_2, "CoCuNb" does not. Further comparisons of the catalytic activities for both types of catalysts are hampered by the very different reaction conditions employed, because Prieto et al.[19] performed their measurements under strictly differential conditions of CO conversion.

The catalytic CO hydrogenation studies of "CoCuNb" as shown above demonstrate that these catalysts may have potential for scale-up in an industrial application to produce
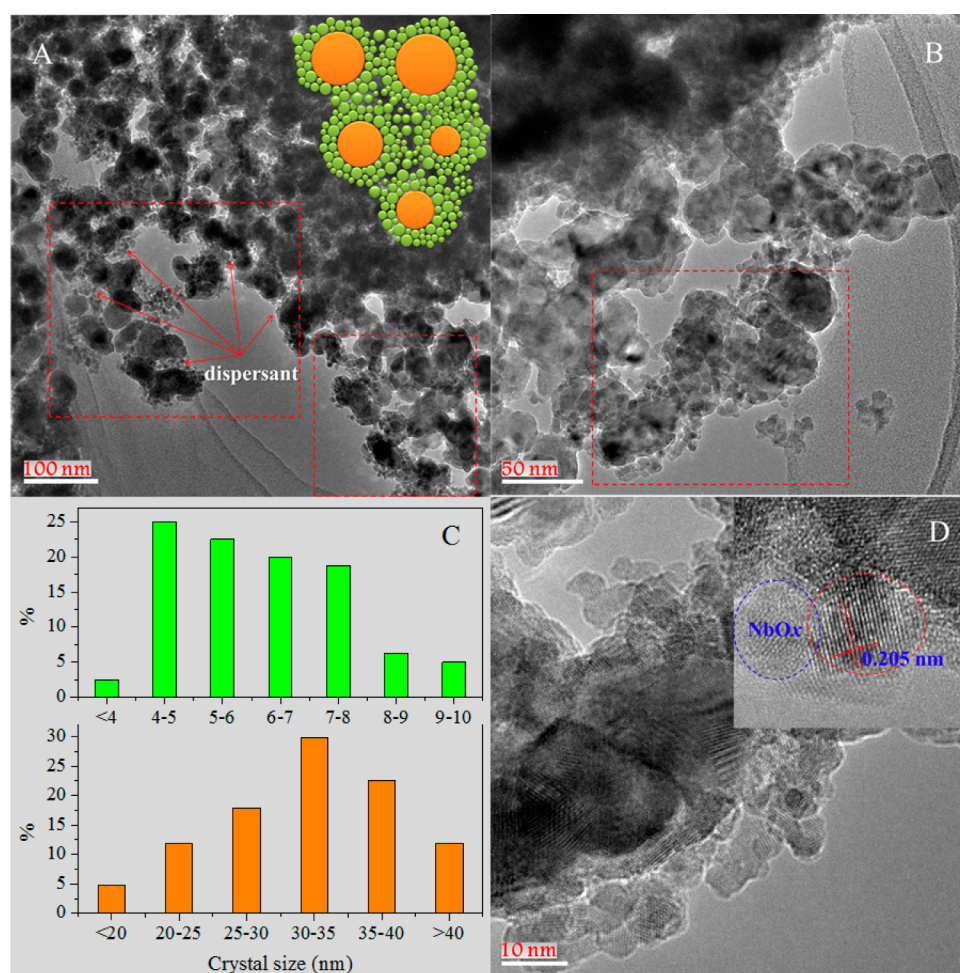

Figure 3. (HR)TEM images of the $Co_2Cu_1Nb_{0.2}$ catalysts (A, B, and D). The inset of (A) provides a model of the bimodal catalyst structure as mounted on the basis of the selected regions in images (A) and (B). (C) Particle size distribution for "CoCu" and "Nb" spacer particles.

higher alcohols as "alkanol" fuels, fuel additives, or precursors for short-chain 1-olefins. The catalytic performance must be associated with the Nb promotion and the "oxalate route" of catalyst preparation, which was shown to result in CoCu polymeric mixed-oxalate structures[13,15] at the instant of precipitation. A similar coprecipitation seemed to apply to ternary "CoCuMn".[3b] H_2-assisted temperature-programmed decomposition (H_2-TPDec) of the "mixed-oxalate" precursors in the present study also indicates the formation of "CoCu" or "CoCuNb" "mixed" structures (see Figure S4 in the Supporting Information).

To explain the beneficial role of Nb in "CoCuNb" catalyst formulations, (HR)TEM (high-resolution transmission electron microscopy) and X-ray photoelectron microscopy (XPS) were employed for various catalyst compositions (although $Co_1Cu_2Nb_{0.2}$ may have advantages over others, the general TEM and XPS features of "CoCuNb" vary little from one specific composition to the other). Figure 3 shows (HR)TEM results for $Co_2Cu_1Nb_{0.2}$ after H_2-TPDec. Generally, most of the particles appear overlapped, which is expected for metallic catalysts in the absence of a generic support material. Specifically, the TEM images (Figure 3A–D) clearly demonstrate the occurrence of a bimodal particle size distribution. The size of the larger CoCu particles is in the range 25–40 nm, peaking at 30–35 nm, and thus covering the average size of 34 nm as determined from measurements of the specific surface area S_{BET} for binary Co_2Cu_1. Quite differently, the minority component, Nb, shows up in particles with smaller size ranging from 4 to 8 nm. The TEM images suggest that these particles act as "spacer" specimen enfolding the larger CoCu particles and thus conferring to "CoCuNb" catalysts a considerable increase in the specific surface area, S_{BET} (for a comparison of TEM images between "CoCu" and "CoCuNb", see Figure S5 in the Supporting Information). By way of example, S_{BET} increases from 20.4 to 49.6 m²/g by adding $Nb_{0.2}$ to Co_2Cu_1. S_{BET} values larger than 110 m²/g are observed for $Co_2Cu_1Nb_{\geq 0.6}$ and Co_2Nb_1. The data are summarized in Table S2 in the Supporting Information.

Although it seems clear that the "spacer" particles ensure a high dispersion of the CoCu particles, the local chemistry cannot be elucidated by merely inspecting our HRTEM images and evaluating fast Fourier transforms (FFT) of specific features. As will be shown below through our XPS results, "Nb" spacer particles are associated with Nb oxides, NbO_x, thus giving rise to the possibility of a synergistic SMSI effect through interaction with metallic sites.[21] Indeed, as seen in Figure 3 and more particularly in Figure 3D (inset), lattice spacings of ~0.205 nm, attributed to the (111) plane of face-centered cubic (fcc) Co or Cu (a distinction is difficult because of the similarity of these metals' lattice constants), can be identified in close proximity to NbO_x "spacer" particles. On the other hand, hexagonal close-packed (hcp) Co can be unequivocally identified (see Figure S6 in the Supporting Information).

To further characterize the Nb oxide phase in "CoCuNb", we present XPS spectra for Nb 3d excitations in Figure 4. $Co_1Cu_1Nb_1$ and $Co_1Cu_1Nb_{0.4}$, which may be regarded as representative for "CoCuNb" formulations, were used in these studies. As can be seen from Figure 4, Nb^{4+} and Nb^{5+} oxidation states are both detected in variable amounts. More precisely, the 3d peak deconvolution clearly shows the relative portion of Nb^{4+} to increase when the Nb nominal amount in "CoCuNb$_x$" is lowered. We therefore conclude that Nb does not reach the 5+ oxidation state in catalysts prepared via oxalate precipitation
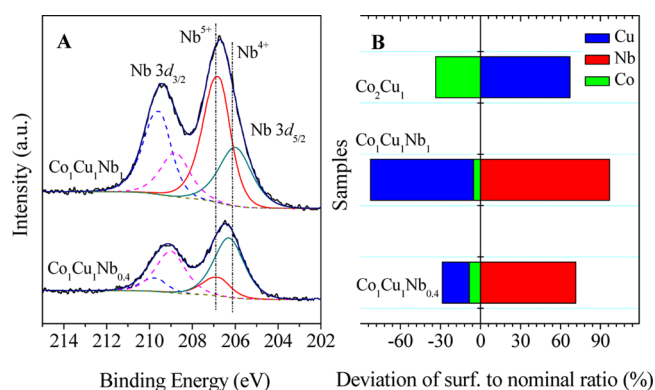

Figure 4. (A) XPS (Nb 3d) spectra of $Co_1Cu_1Nb_1$ and $Co_1Cu_1Nb_{0.4}$ as examples of "CoCuNb" formulations. (B) Deviations of surface Co, Cu, and Nb relative amounts (from XPS) to their corresponding nominal amounts in bulk samples, defined as $(\delta(i)_{surface} - \delta(i)_{nominal})/\delta(i)_{nominal} \times 100\%$, where $\delta(i)$ represents the relative amount of an atom. Co_2Cu_1 atomic surface deviations are added from ref 15.

and decomposition. Nominal amounts of Nb with $x < 1$ (for Co/Cu ratios ≤2), which may have advantages when it comes to increasing the selectivity of alcohol production, tend to contain more NbO_2 instead. According to the classical concepts provided by Tauster et al.,[21] the occurrence of reduced oxidation states in metal oxides with variable stoichiometry is mandatory to provoke SMSI behavior. An electron transfer from reduced surface cations, Nb^{4+} in our case, to the metallic (CoCu) phase was invoked, possibly leading to the formation of a Schottky barrier at the metal oxide/metal interface. The occurrence of SMSI effects was also reported for Co/Nb_2O_5 catalysts in which Nb_2O_5 was used as a generic support material and shown to transform into NbO_2 under reducing conditions.[22]

Another interesting observation from our XPS studies is associated with the significant changes in the surface composition when Nb amounts are added to "CoCu". Deviations of surface Co, Cu, and Nb amounts relative to the corresponding nominal bulk composition are shown in Figure 4B (see Table S3 in the Supporting Information for a detailed relative surface composition). Data were compared with those of Co_2Cu_1 published previously.[15] As can be seen, while the surface abundance of Cu largely exceeds its bulk value in Co_2Cu_1, the reverse is true for "CoCuNb": both $Co_1Cu_1Nb_{0.4}$ and $Co_1Cu_1Nb_1$ formulations show a large suppression in the Cu surface abundance. Instead, a pronounced excess of Nb is observed. This is in accordance with our TEM observations and supports the view that NbO_x aggregates tend to spread over the metallic particle surfaces. It must be concluded that the Co@Cu core−shell structure as present in "CoCu" binary[15] and "CoCuMn" ternary[3b] formulations are not maintained in CoCuNbO$_x$. We may also speculate that the intrinsic electron transfer operating the SMSI effect involves Nb^{4+} states in NbO_x and metallic Co, rather than Cu. A NbO_x-induced Co segregation would also be in accordance with $Co_2Nb_5O_{14}$ or $CoNb_2O_6$ formation, as reported previously in studies with Co/Nb_2O_5 catalysts.[22]

■ CONCLUSION

To summarize, we have demonstrated that ternary "CoCuNb" catalysts prepared through the "oxalate route" show high selectivity in C_2−C_5 alcohol formation during CO hydro-

genation. Quite different from a classical catalyst with metal particles on a generic support, "CoCuNb" formulations show a bimodal nanosized particle distribution. Co−Cu metallic particles are larger than NbO_x "spacer particles". The range extends from 25 to 40 nm and from 4 to 8 nm, respectively. The smaller NbO_x "spacers" not only enhance the BET specific surface area significantly (from 20 to up to 120 m^2/g) but also cause the surface concentration of Co to increase relative to Cu in "CoCu". A 4+ oxidation state for Nb in NbO_x was identified. Such NbO_x particles tend to spread across the CoCu metallic particles, thus giving rise to the possibility of an SMSI effect.

With respect to the catalytic CO hydrogenation performance, "CoCuNb" catalysts show that the total primary alcohol selectivity (including CO_2) reaches ~50 wt %, with the combined primary alcohol/alkene selectivity hitting ~73 wt %. The α-ASF chain lengthening probabilities for alcohols at reaction temperatures between 180 and 240 °C demonstrate that $C_2−C_5$ primary alcohols attain up to 75% of the entire alcohol slate. This performance feature is very different from that obtained for our "CoCuMn"[3b] and "CoCuMo"[20] ternary formulations, which targeted the optimization of long-chain $C_8−C_{14}$ alcohol production. CO conversion with all "CoCu"-based catalysts under low-temperature reaction conditions remains below 20%. While it may seem appropriate to develop catalyst formulations providing higher activities, one has to keep in mind the considerable exothermicity of the process and the need to develop suitable means for managing the heat removal from the reactor.

■ ASSOCIATED CONTENT

Ⓢ Supporting Information

The following file is available free of charge on the ACS Publications website at DOI: 10.1021/acscatal.5b00388.

Tables S1−S2 and Figures S1−S7, as described in the text (PDF)

■ AUTHOR INFORMATION

Corresponding Author

*E-mail for N.K.: Norbert.Kruse@wsu.edu.

Notes

The authors declare no competing financial interest.

■ ACKNOWLEDGMENTS

■ REFERENCES

(1) Roelen, O. Chemische Verwertungsgesellschaft m.b.H., (Oberhausen-Holten), DE 849548, 1938.

(2) Heck, R. F.; Breslow, D. S. *J. Am. Chem. Soc.* **1961**, *83*, 4023−4027.

(3) (a) Buess, P.; Caers, R. F. I.; Frennet, A.; Ghenne, E.; Hubert, C.; Kruse, N. US 6362239 B l, 2002. (b) Xiang, Y.; Chitry, V.; Liddicoat, P.; Felfer, P.; Cairney, J.; Ringer, S.; Kruse, N. *J. Am. Chem. Soc.* **2013**, *135*, 7114−7117.

(4) (a) Khodakov, A. Y.; Chu, W.; Fongarland, P. *Chem. Rev.* **2007**, *107*, 1692−1744. (b) Ojeda, M.; Nabar, R.; Nilekar, A. U.; Ishikawa, A.; Mavrikakis, M.; Iglesia, E. *J. Catal.* **2010**, *272*, 287−297. (c) van Santen, R. A.; Ciobica, I. M.; van Steen, E.; Ghouri, M. M. *Adv. Catal.* **2011**, *54*, 127−187 DOI: 10.1016/B978-0-12-387772-7.00003-4.

(5) Schweicher, J.; Bundhoo, A.; Frennet, A.; Kruse, N.; Daly, H.; Meunier, F. D. R. C. *J. Phys. Chem. C* **2010**, *114*, 2248−2255.

(6) (a) Melaet, G.; Ralston, W. T.; Li, C.-S.; Alayoglu, S.; An, K.; Musselwhite, N.; Kalkan, B.; Somorjai, G. A. *J. Am. Chem. Soc.* **2014**, *136*, 2260−2263. (b) Lancelot, C.; Ordomsky, V. V.; Stéphan, O.; Sadeqzadeh, M.; Karaca, H.; Lacroix, M.; Curulla-Ferré, D.; Luck, F.; Fongarland, P.; Griboval-Constant, A.; Khodakov, A. Y. *ACS Catal.* **2014**, *4*, 4510−4515.

(7) Fischer, F.; Tropsch, H. *Brennst. Chem.* **1923**, *4*, 276−285.

(8) (a) Frolich, P. K.; Lewis, W. K. *Ind. Eng. Chem.* **1928**, *20*, 354−359. (b) Graves, G. D. *Ind. Eng. Chem.* **1931**, *23*, 1381−1385. (c) Wenzel, W. *Angew. Chem.* **1948**, *20*, 225−231. (d) Anderson, R. B.; Feldman, J.; Storch, H. H. *Ind. Eng. Chem.* **1952**, *44*, 2418−2424. (e) Natta, G.; Colombo, V.; Pasquon, I. In *Catalysis*; Emmet, P. H., Ed.; Reinhold: New York, 1957; Vol. *V*, pp 131−174.

(9) Courty, P.; Durand, D.; Freund, E.; Sugier, A. *J. Mol. Catal.* **1982**, *17*, 241−254.

(10) (a) Sugier, A.; Freund, E. US 4122110, 1978. (b) Sugier, A.; Freund, E. US 4291126, 1981. (c) Sugier, A.; Freund, E. US 4346179, 1982. (d) Chang, C. D.; Perkins, P. D. US 4440668, 1984. (e) Nay, B.; Stewart, D. G. US4567160, 1986. (f) Courty, P.; Durand, D.; Sugier, A.; Freund, E. US 4659742, 1987. (g) Courty, P.; Chaumette, P.; Durand, D.; Verdon, C. US 4780481, 1988.

(11) (a) Xiaoding, X.; Doesburg, E. B. M.; Scholten, J. J. F. *Catal. Today* **1987**, *2*, 125−170. (b) Baker, J. E.; Burch, R.; Golunski, S. E. *Appl. Catal.* **1989**, *53*, 279−297. (c) Mouaddib, N.; Perrichon, V.; Martin, G. A. *Appl. Catal., A* **1994**, *118*, 63−72.

(12) (a) Subramanian, N. D.; Balaji, G.; Kumar, C. S. S. R.; Spivey, J. J. *Catal. Today* **2009**, *147*, 100−106. (b) Mo, X.; Tsai, Y.-T.; Gao, J.; Mao, D.; Goodwin, J. G., Jr *J. Catal.* **2012**, *285*, 208−215. (c) Tsai, Y.-T.; Mo, X.; Goodwin, J. G., Jr *J. Catal.* **2012**, *285*, 242−250. (d) Wang, J.; Chernavskii, P. A.; Khodakov, A. Y.; Wang, Y. *J. Catal.* **2012**, *286*, 51−61.

(13) Donia, A. M.; Dollimore, D. *Thermochim. Acta* **1997**, *290*, 139−147.

(14) (a) Silva, R. R. C. M.; Schmal, M.; Frety, R.; Dalmon, J. A. *J. Chem. Soc., Faraday Trans.* **1993**, *89*, 3975−3980. (b) Mendes, F. M. T.; Perez, C. A. C.; Noronha, F. B.; Schmal, M. *Catal. Today* **2005**, *101*, 45−50. (c) Ito, S.-I.; Fujimori, T.; Nagashima, K.; Yuzaki, K.; Kunimori, K. *Catal. Today* **2000**, *57*, 247−254. (d) den Otter, J.; de Jong, K. *Top. Catal.* **2014**, *57*, 445−450.

(15) Xiang, Y.; Barbosa, R.; Kruse, N. *ACS Catal.* **2014**, *4*, 2792−2800.

(16) Dong, G.; Teo, P.; Wickens, Z. K.; Grubbs, R. H. *Science* **2011**, *333*, 1609−1612.

(17) (a) Guerbet, M. *Ann. Chim. Phys.* **1902**, *27*, 67−105. (b) Frolich, P.; Cryder, D. *Ind. Eng. Chem.* **1930**, *22*, 1051−1057. (c) Kozlowski, J. T.; Davis, R. J. *ACS Catal.* **2013**, *3*, 1588−1600.

(18) (a) Kuipers, E. W.; Vinkenburg, I. H.; Oosterbeek, H. *J. Catal.* **1995**, *152*, 137−146. (b) Kuipers, E. W.; Scheper, C.; Wilson, J. H.; Vinkenburg, I. H.; Oosterbeek, H. *J. Catal.* **1996**, *158*, 288−300. (c) Iglesia, E. *Appl. Catal., A* **1997**, *161*, 59−78. (d) . (b) Van Der Laan, G. P.; Beenackers, A. A. C. M. *Catal. Rev.: Sci. Eng.* **1999**, *41*, 255−318. (e) Schulz, H.; Claeys, M. *Appl. Catal., A* **1999**, *186*, 71−90.

(19) Prieto, G.; Beijer, S.; Smith, M. L.; He, M.; Au, Y.; Wang, Z.; Bruce, D. A.; de Jong, K. P.; Spivey, J. J.; de Jongh, P. E. *Angew. Chem., Int. Ed.* **2014**, *53*, 6397−6401.

(20) Xiang, Y.; Chitry, V.; Kruse, N. *Catal. Lett.* **2013**, *143*, 936−941.

(21) Tauster, S. J.; Fung, S. C.; Baker, R. T. K.; Horsley, J. A. *Science* **1981**, *211*, 1121−1125.

(22) Noronha, F. B.; Perez, C. A.; Schmal, M.; Frety, R. *Phys. Chem. Chem. Phys.* **1999**, *1*, 2861−2867.